Nuclear Instruments and Methods in Physics Research A 654 (2011) 604–607

Contents lists available at ScienceDirect

Nuclear Instruments and Methods in Physics Research A

journal homepage: www.elsevier.com/locate/nima

Application of a double-sided silicon-strip detector as a differential pumping barrier for NESR experiments at FAIR

B. Streicher [a,b,*], P. Egelhof [b], S. Ilieva [b], N. Kalantar-Nayestanaki [a], H. Kollmus [b], Th. Kröll [c], M. Mutterer [b,c], M. von Schmid [c], M. Träger [b]

[a] KVI, University of Groningen, Zernikelaan 25, 9747AA Groningen, The Netherlands
[b] GSI Helmholtz Centre for Heavy Ion Research, Planckstraße 1, 64291 Darmstadt, Germany
[c] Institute of Nuclear Physics, University of Technology, Schlossgartenstraße 9, 64289 Darmstadt, Germany

ARTICLE INFO

Article history:
Received 6 January 2011
Received in revised form
26 May 2011
Accepted 16 June 2011
Available online 24 June 2011

Keywords:
Double-sided silicon-strip detector
Differential vacuum
Storage ring

ABSTRACT

The presented work focuses on the development of a differential pumping system using double-sided silicon-strip detectors to separate the ultra-high vacuum of a storage ring from subsequent detectors and outgassing components placed in an auxiliary vacuum. Such a technical concept will give the opportunity to use telescope-like detector systems in an ultra-high vacuum environment, such as a storage ring, without enclosing the entire system in a pocket. Therefore, it will enable the detection of recoil particles with the smallest possible energy due to the use of the innermost strip detector as an active window. Our results prove that such an assembly is feasible without having an effect, within experimental errors, on the performance of the strip detector. Vacuum separation better than six orders of magnitude was achieved with the ultra-high vacuum side reaching down to the 10^{-10} mbar pressure region.

1. Introduction

The project EXotic nuclei studied in Light ion induced reactions (EXL) [1] at the New Experimental Storage Ring (NESR) as a part of the future FAIR [2] facility will provide the means for studying many physics phenomena in unstable nuclei. Reactions will be studied in inverse kinematics using new storage-ring techniques and a universal detector system providing high resolution and large solid angle coverage for kinematically complete measurements (see Refs. [3,4] for the first feasibility tests of the concept).

The crucial part of EXL lies in the successful development of the EXL Silicon Particle Array (ESPA). This detector array consists of telescope-like segments which, depending on the angular range in ESPA, can house up to two Double-sided Silicon-Strip Detectors (DSSDs), two Si(Li) detectors and a CsI scintillator crystal. The innermost DSSDs are common for all the segments and will be arranged in a spherical configuration.

The greatest technical challenge is to install all the detectors with the corresponding Front-End Electronics (FEE), connectors, cabling and cooling circuits at the beam-target interaction region of the NESR where vacuum of the order of 10^{-10} mbar or below is required. In order to achieve such vacuum conditions it is necessary to bake all the installed equipment. The baking temperature starts at the minimum value of 120 °C going up to 250 °C to reduce the bake-out time to a couple of days. The bake-out puts additional constraints on the choice of materials and design for the ESPA construction. To fulfill these requirements a differential pumping concept was proposed by Mutterer [5], where the NESR Ultra-High Vacuum (UHV) is separated from the Auxiliary Vacuum (AV) using the innermost DSSD sphere as a vacuum barrier. In such a design, the subsequent layers of DSSDs and/or Si(Li) detectors, together with all unbakeable and thus outgassing components are placed in the AV where the constraints on the vacuum are at least three orders of magnitude less stringent. Since the vacuum barrier serves at the same time the purpose of an active window it also enables the detection of recoil particles varying from protons to alphas with low energy, down to about 100 keV, as a result of a low momentum transfer. The development, construction and testing of such a prototype vacuum window was carried out at GSI, Darmstadt and is described in the subsequent sections.

2. Technical concept

2.1. Detector sensor

The DSSD sensor with an active area of 19×19 mm^2 used in our prototype [6] was designed at PTI, Petersburg [7], and processed on high resistivity (7−20 kΩ cm) n-type silicon wafers

* Corresponding author at: GSI Helmholtz Centre for Heavy Ion Research GmbH, Planckstraße 1, 64291 Darmstadt, Germany.
Tel.: +49 6159 71 2650; fax: +49 6159 71 2809.
E-mail address: b.streicher@gsi.de (B. Streicher).

0168-9002/$ - see front matter © 2011 Elsevier B.V. All rights reserved.
doi:10.1016/j.nima.2011.06.075

of $285 \pm 10\,\mu m$ thickness grown in orientation $\langle 1\,0\,0 \rangle$. Each detector side has 64 strips of 19 mm length. The strips on the two sides are perpendicular to each other. The strips on the p^+ side are on a 300 μm pitch with a 15 μm interstrip gap passivated with a SiO_2 layer. Instead of a continuous metalization layer only a narrow aluminum frame around each strip is used for electrical contact. The n^+ side has strips on the same pitch, but with a wider interstrip gap of 85 μm filled with p^+ implants used to enhance interstrip insulation. Both detector sides were read out using AC-coupled preamplifiers. The negative bias to the DSSD was applied through each channel of the p^+ side. This side also triggered the acquisition system using an OR of all the channels. The minimum value of the total depletion voltage was established at -46 V considering the lower limit of the silicon resistivity of 7 kΩ cm, but an over-bias of up to -120 V was applied to reduce the charge collection time and thus to enhance the performance of the fast output of the preamplifiers used for the trigger. The preamplifiers on the n^+ side were grounded through a 50 Ω resistor. Each side of the DSSD was read out by 16 data channels with four neighboring strips on the DSSD coupled together. The shaping time of the main amplifier was set to 1 μs for each channel.

2.2. PCB and connectors

The Printed Circuit Board (PCB) for the read out of the detector was designed at GSI and manufactured by LUST Hybrid-Technik GmbH [8] from aluminum nitride (AlN) ceramic. This material was chosen for its low outgassing, good dielectric properties, high thermal conductivity and thermal expansion coefficient close to that of silicon. The transmission mount design of the PCB is shown in Fig. 1. It has 16 printed gold signal lines for every side of the detector. The signal lines from the PCB side facing the UHV pass through the AlN material via laser-drilled holes covered with a glass layer to assure vacuum tightness. This ensures that the UHV side consists entirely of UHV compatible materials such as the AlN board with golden printed lines, the DSSD and the aluminum bonding wires all of which have low outgassing and can be subjected to baking. The DSSD sensor was hermetically glued in a laser-cut step, seen in the detail cut of Fig. 1, using a low-outgassing EPO-TEK H77 [9] two-component glue which has a total mass loss less than 0.06% at 200 °C. The detector strips were manually bonded to the bonding pads printed on the PCB, grouping four neighboring channels to a single pad.

Custom made connectors were manufactured using PEEK® material which is well machinable and can withstand the temperature required for the bake-out procedure. They were mechanically fixed on the stainless steel cover flange (see Section 2.3) rather than on the PCB. The connection to the signal traces on the PCB was accomplished by spring-pin probes [10] that touched the circular printed pads on the PCB and, on the other side, were glued to the cable lines using EPO-TEK H22 conductive glue. The minimum contact area to the PCB and the thin walls of these tube-like probes minimize the heat transfer to the connector and subsequent cables during the bake-out process.

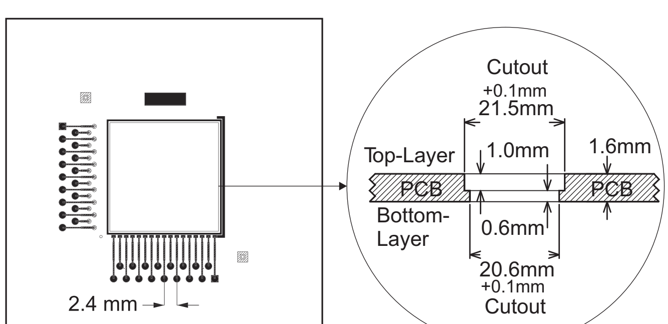

Fig. 1. Layout of the printed circuit board made from AlN material. The two horizontal and two vertical rows of the signal pads are bonded to the n-side and the p-side of the DSSD, respectively (for clarity, the DSSD is not shown). The cross-sectional view on the right side shows a detail of an opening onto which the DSSD sensor is glued.

2.3. DSSD active window prototype and vacuum test stand

The idea of using DSSDs as a vacuum barrier to separate the storage ring vacuum from the auxiliary vacuum was realized in a small test vacuum chamber divided into two parts and separated by a custom machined CF150 flange with an opening of $4 \times 4\,cm^2$ in the middle, as shown in Fig. 2. The PCB was installed over this opening using another steel top frame and two rings made of aluminum wires of 1.5 mm diameter. On each side of the PCB one ring was installed in order to minimize the mechanical forces acting on the PCB during the baking, however, only the bottom one served the purpose of a vacuum seal. A small groove of 0.3 mm height was machined around the opening on the CF150 flange, as well as on the top frame, to hold both seals in place (Fig. 2b). The top frame was tightened with 16 M5 screws using disc spring washers enabling one to press the PCB between the aluminum seals with a known force of 12 ± 2 N/mm of wire length. The top frame was situated on the AV side and attached to it were the connectors to read both sides of the DSSD. The detector was tested using an ^{241}Am α source also mounted on the AV side in order to avoid its excessive heating. It was enclosed in an aluminum holder screwed onto the CF150 flange.

The vacuum test stand is schematically shown in Fig. 3. Each side was equipped with a TurboMolecular Pump (TMP) with a

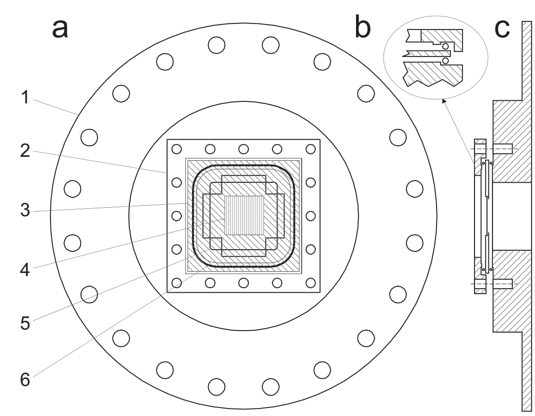

Fig. 2. (a) Schematic drawing of the test flange that separated the two vacuum chambers and onto which the ceramic PCB was mounted: 1—CF150 flange, 2—top frame, 3—PCB, 4—DSSD, 5—opening in CF150 flange, 6—aluminum ring; (b) detail of the grooves holding the wires; and (c) cross-section of the test flange. The α-source holder and the mounting holes for the connectors are not shown for the sake of clarity.

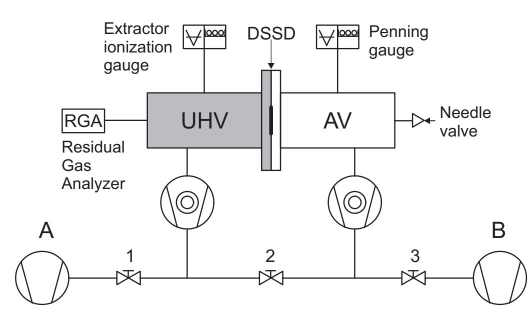

Fig. 3. Block diagram of the setup for the differential vacuum test. The shaded part of the chamber was wrapped in a heating jacket and baked out at 150 °C in order to reach UHV.

pumping speed of 250 l/s coupled through CF100 flanges. The pre-pump A was a combination of an oil-free membrane pump with a TMP. The combination was used as a booster for the next TMP. The pre-pump B was a rotary vane pump. First, both sides were pumped in parallel by pre-pump A with valves 1 and 2 opened and valve 3 closed. After reaching a vacuum of 5×10^{-3} mbar valve 2 was closed, valve 3 opened and both sides were pumped separately using their own TMPs. In this configuration the only interplay between the two chambers was through the installed PCB holding the detector. After that the UHV side was gradually baked with heating jackets up to 150 °C during a period of 2 days in order to remove water and other trace gases which were adsorbed on the surfaces of the chamber and the PCB-DSSD barrier. Following the bake-out the temperature was ramped down in one day to reach room temperature.

3. Measurements and results

After the bake-out, on the UHV side the vacuum reached the value of 1.2×10^{-10} mbar, which was the limit of the installed TMP for the given conductance through a CF100 flange. The corresponding vacuum on the AV side was 2.2×10^{-7} mbar. Using the needle valve (Fig. 3) we introduced an artificial air leak on the AV side to observe its influence on the UHV side through the PCB-DSSD barrier. The results are shown in Fig. 4. Very stable vacuum conditions were maintained on the UHV side. While the pressure on the AV side increased due to the leak over a range greater than four orders of magnitude, the pressure on the UHV side increased by less than a factor of three, staying well within the achieved 10^{-10} mbar range. Thus, we have established that the DSSD, used as a differential vacuum barrier, can maintain a difference in the vacuum between both sides of the barrier of up to six orders of magnitude.

Outgassing spectra were measured on the UHV side with a residual gas analyzer for two cases: before the leak on the AV side was introduced and with a maximum leak. The results are shown in Fig. 5. The spectrum has the typical features of an air leak and it is free of organic compounds. The most pronounced increase was detected in molecular and atomic nitrogen, molecular oxygen as well as argon, which are the basic air constituents.

At the end of the bake-out and vacuum tests a measurement of the DSSD performance was done using injection of ^{241}Am α particles. The idea was to check whether the PCB-DSSD system can withstand the bake-out procedure and the mechanical forces introduced by the temperature change and to evaluate their influence on the spectroscopic performance. The injection from the n^+ side was chosen since the α source could not be placed in the baked environment of the UHV chamber. Because injection of α particles from the n^+ side results in a degraded resolution for our type of DSSD compared to injection from the p^+ side, only a basic functionality check was done proving that all 16+16 channels were fully operational. However, two supplementary measurements, one before and one after the bake-out and vacuum tests, were performed in a different non-UHV chamber using the p^+ injection to investigate the influence of the bake-out cycle on the DSSD performance. The moderate vacuum condition of $\sim10^{-4}$ mbar, sufficient for such spectroscopy tests, were used in both measurements with no pressure difference between the two faces of the DSSD. The results presented in Fig. 6 show the ^{241}Am α spectrum before and after the baking. The difference in resolution between the two cases cannot be attributed to degradation of detector properties, but merely to different noise conditions during the measurement. The basic properties such as the detector leakage current, in our case of the order of few tens of pA, as well as signal rise time and amplitude after the preamplifier remained unchanged within the margin of the

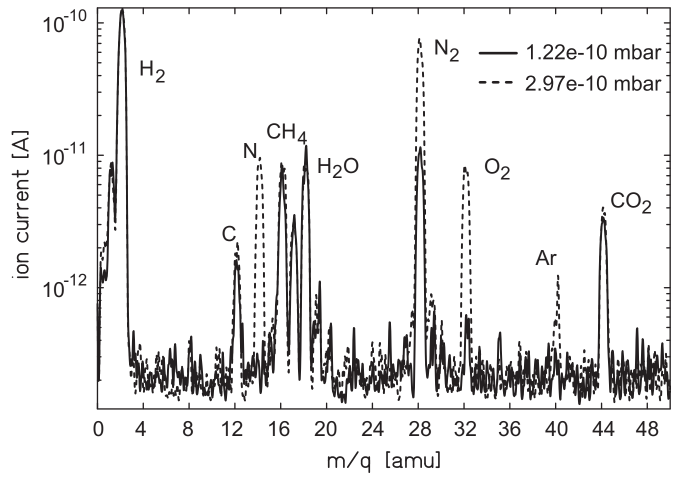

Fig. 5. Outgassing spectra taken at the UHV side of the chamber with the residual gas analyzer. The solid curve shows the residual gas spectrum when no leak was present and the dotted curve the one after the leak at the AV side reached its maximum value.

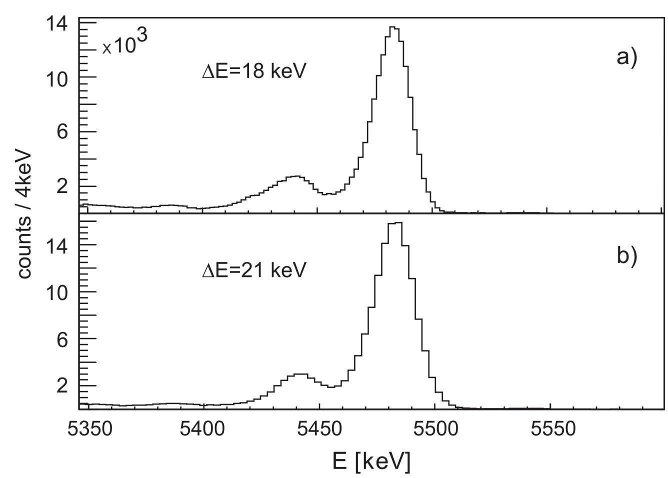

Fig. 6. Energy spectrum of a single strip for the p^+ injection of ^{241}Am α particles measured: (a) before the baking and (b) after the baking. Resolution values are given as FWHM.

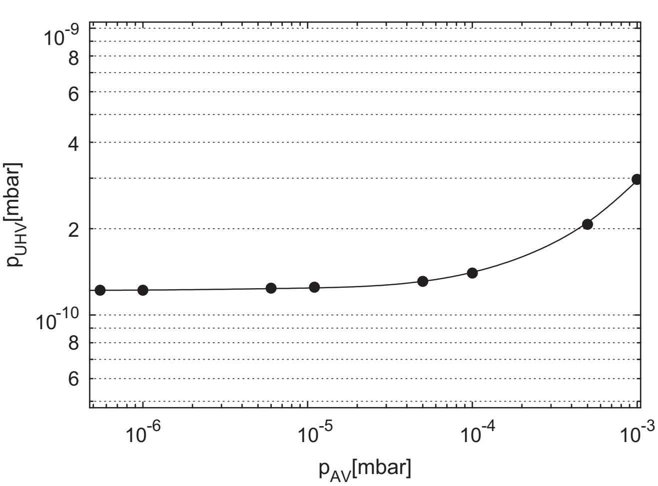

Fig. 4. Dependence of the pressure on the UHV side on the AV side pressure influenced by an air leak artificially introduced through the needle valve installed on the AV side (see Fig. 3).

experimental error. Therefore, we claim that the DSSD characteristics were not influenced by the bake-out cycle and the energy resolution values for the p^+ injection achieved before and after the bake-out cycle coincide within the uncertainty of the measurement.

4. Future perspectives

For the accepted experimental proposal E105 at the existing storage ring at GSI, where we aim to perform the experiments with stable and close to stability radioactive beams already at the present storage ring, we need to construct a new detector of $64 \times 64\,mm^2$ active area with 128 and 64 strips on p^+ and n^+ side, respectively, on a corresponding AlN PCB utilizing the described differential vacuum technique. The size and number of strips of this DSSD represent the detector adequate for the final EXL design. In order to guarantee the mechanical stability, to minimize sheer stress and to use even lower pressing power we intend to use high quality Helicoflex® [11] rings that lack the welded joint of the currently used aluminum rings, are very planar and have small and well defined contact surface. The surface quality of the PCB will also be improved to have surface smoothness on the order of 0.5 μm and planarity of 50 μm compared to the guaranteed values of 4−6 μm and 250 μm, respectively, for the present PCB.

5. Conclusions

The aforementioned prototyping was done in the frame of R&D for the EXL project in order to insure that the experimental concept, namely using a stack of detectors in the UHV environment, is feasible. Our test results demonstrate the possibility of operating a differential vacuum system in the storage ring environment using DSSDs as a vacuum barrier. It was shown that the PCB-DSSD system withstands the bake-out cycle and the mechanical sheer stresses connected with the thermal expansion with unchanged spectroscopy performance, within the experimental errors. Chosen materials facing the UHV environment proved to be clean of any UHV disturbing contaminants. The achieved vacuum difference ranged over more than six orders of magnitude with the vacuum on the UHV side staying well within the 10^{-10} mbar range, which is an acceptable vacuum for the interaction region with internal target at the storage ring.

It shall be noted that the concept of this development can be potentially applied outside of the EXL project for experiments at storage rings requiring the usage of DSSDs in UHV. Due to the fact that the entrance detector serves the purpose of an active window, telescope-like detector configurations used in the UHV can measure low-energy particles of about 100 keV as well as penetrating particles with energies of several hundreds of MeV stopped in subsequent detectors.

Acknowledgements

We want to express our gratitude to Jose Cavaco and Lukas Urban from the GSI vacuum group for their technical support and the GSI mechanical workshop for the precise fabrication of mechanical components. This work was supported in part by BMBF (06DA9040I) and HIC for FAIR.

References

[1] EXL home page: ⟨http://www.rug.nl/kvi/Research/hnp/Research/EXL/index⟩, February 19, 2011.
[2] FAIR homepage: ⟨http://www.fair-center.com⟩, February 19, 2011.
[3] S. Ilieva, et al., Eur. Phys. J. Special Top. 150 (2007) 357.
[4] H. Moeini, S. Ilieva, et al., Nucl. Instr. and Meth. A 634 (2011) 77.
[5] Proposed at the Joint R³B/EXL/ELISe Collaboration Meeting on Technical Issues, GSI, April 21–24, 2008.
[6] B. Streicher, et al., GSI Sci. Rep. 2008-1 (2008) 55.
[7] V. Eremin, Private communication.
[8] PCB manufacturer: ⟨http://www.lust-hybrid.de⟩, February 19, 2011.
[9] Glue producer: ⟨http://www.epotek.com⟩, February 19, 2011.
[10] Spring pin producer: ⟨http://www.idinet.com ⟩, February 19, 2011.
[11] Seal producer: ⟨http://www.helicoflex.com⟩, February 19, 2011.